A NUMERICAL STUDY OF THE MICROWAVE INSTABILITY AT APS*

A. Blednykh#, G. Bassi, V. Smaluk, BNL, NSLS-II, Upton, NY, 11973-5000, USA
R. R. Lindberg, ANL, Argonne, IL 60439, USA

Abstract

Two particle tracking codes, ELEGANT and SPACE, have been used to simulate the microwave instability in the APS storage ring. The total longitudinal wakepotential for the APS vacuum components, computed by GdfidL, has been used as the input file for the simulations. The numerical results have been compared with bunch length and the energy spread measurements for different single-bunch intensities.

LONGITUDINAL MICROWAVE INSTABILITY

In this paper we compare the results of numerical simulations obtained using the ELEGANT [1] and SPACE [2] codes with measurements taken at the APS storage ring. The main parameters of the APS storage ring are shown in Table 1.

Table 1: Main APS Storage Ring Parameters [3]

Energy	$E[GeV]$	7
Revolution Period	$T_0[\mu s]$	3.682
Momentum Compaction	α	2.82×10^{-4}
Energy Loss	$U\ [MeV]$	5.353
RF Voltage	$V\ [MV]$	9
Synchrotron Tune	ν_s	0.0078
Damping Time	$\tau_{x,y/s}\ [ms]$	9.6/4.8
Energy Spread	$\sigma_{\varepsilon 0}\ [\%]$	0.096
Bunch Length	$\sigma_{t0}\ [ps]$	20

The total longitudinal wakepotential has been computed by the GdfidL code [4] for the APS vacuum components distributed around the ring. The longitudinal wakepotential for a 1mm bunch length is shown in Fig. 1. This wakepotential was simulated by Y.-C. Chae, it reflects contribution from most of the components. Based on the geometry complexity the step size for the simulations with GdfidL was probably varied, which can affect the accuracy of the simulations for different geometries. The obtained wakepotential is used to determine the instability thresholds and the numerical results are compared with the measurements. The longitudinal impedance is shown in Fig. 2 up to 150GHz. It should be noted here, that the measured results can be confirmed numerically using the numerically simulated by Y.-C. Chae the wakepotential for a shorter bunch length, 10 times shorter, than the circulating bunch in the storage ring (at low current) for longitudinal and transverse instabilities [5].

In Figs. 3 and 4 we compare the bunch length and energy spread obtained by two codes numerically with the measurements. The grey trace of Fig. 3 is the experimental fit of the bunch length. The blue and green dots represent the numerical results of SPACE and ELEGANT respectively.

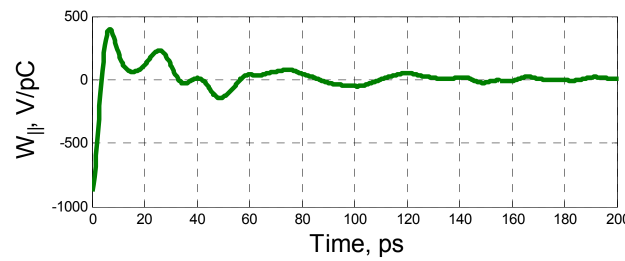

Figure 1: The total longitudinal wakepotential of the APS storage ring simulated for a 1mm bunch length, including the resistive walls and geometric changes of the vacuum components.

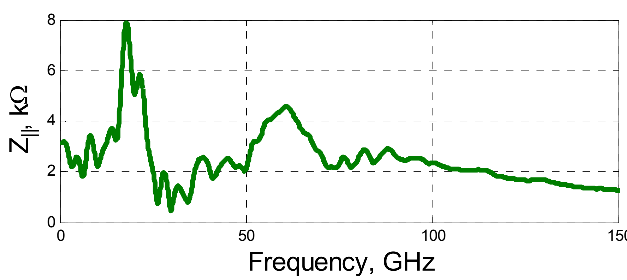

Figure 2: Modulus of the longitudinal impedance obtained by FFT of the longitudinal wakepotential presented in Fig. 1.

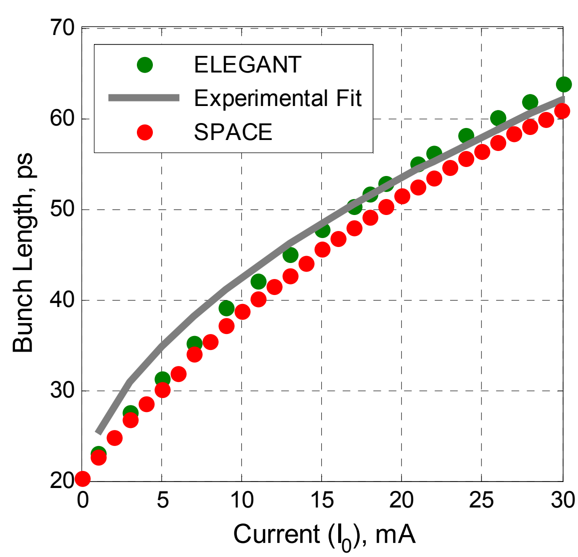

Figure 3: Bunch length vs. single bunch current at $V_{RF} = 9MV$. The experimental results are represented by the experimental fit obtained during several measurements in APS. The green and blue dots correspond to the ELEGANT and SPACE numerical results respectively.

*Work supported by Department of Energy contract DE-AC02-98CH10886 (BNL) and ANL contract is DE-AC02-06CH11357
#blednykh@bnl.gov

In Fig. 4, the energy spread is plotted as a function of single bunch current. The grey dots are from data measured in 2014 at RF voltage 9MV. The numerical results obtained with ELEGANT (green dots) and SPACE (blue dots) agree with each other and describe well the behaviour of the measurements at low and high single-bunch current.

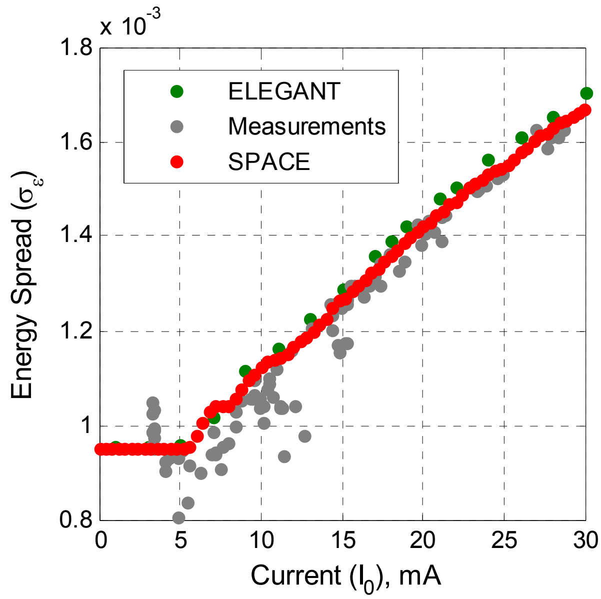

Figure 4: Energy spread vs single bunch current. Comparison of the measured data (grey dots) with the numerical results obtained with the ELEGANT (green dots) and SPACE (blue dots) codes.

The RMS energy spread of the electron beam in APS has been measured at low current in 2001 [6] and in 2005 [7], with values $\sigma_{\varepsilon 0} = 0.91 \times 10^{-3}$ (Fig. 5) and $\sigma_{\varepsilon 0} = 0.96 \times 10^{-3}$ (Fig. 6) respectively. In Fig. 5, three different regions are shown: region I below the microwave instability threshold current $I_{th1} = 7.4mA$, and region II and III above it, where the energy spread increases. Region II and III are separated at the transition threshold $I_{th2} = 8.8mA$, where a change in the functional dependence of the energy spread on the bunch current is observed. The appearance of a change in behaviour of the energy spread increase has been observed at SPEAR II [8] as well. Recent measurements performed at the NSLS-II storage ring, using three different diagnostic methods, have confirmed the same phenomenon by demonstrating the appearance of several transition thresholds in studies of the dependence of the microwave instability threshold on the RF voltage [9]. The physical mechanism responsible for the change in the behaviour of the energy spread increase as a function of current is under investigation. Possible candidates, such as mode mixing at the transition thresholds are being considered [9].

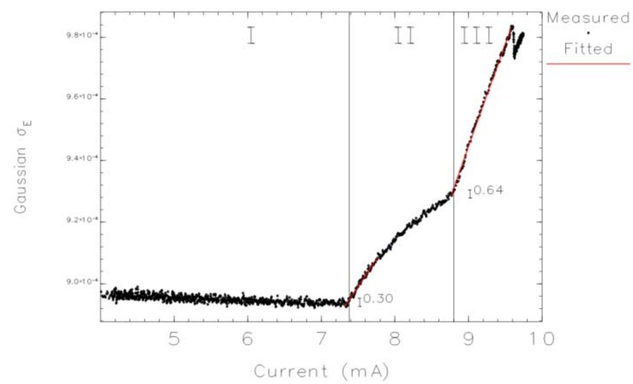

Figure 5: Energy spread vs single bunch current measurements in APS at RF voltage 9.4MV, 2001.

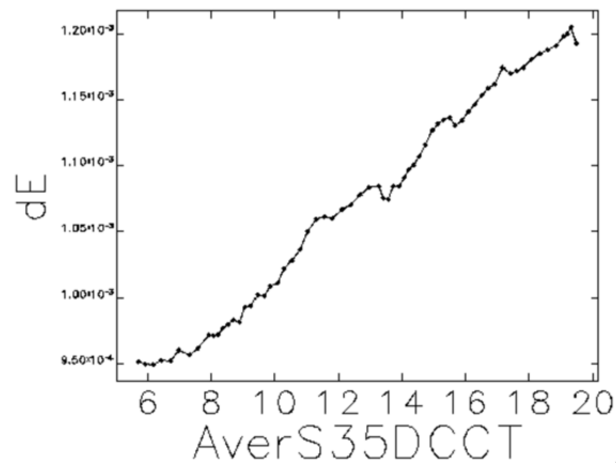

Figure 6: Energy spread vs single bunch current measurements in APS, June 2005 at RF voltage 7MV.

The dependence of the longitudinal instability thresholds on the RF voltage in the APS storage has been studied numerically with SPACE simulations. In Fig. 7, the energy spread vs. single bunch current is plotted for the RF voltage in the range 7MV-15MV. For a clearer interpretation of the results, the data are separated uniformly by the quantity $\Delta = 10^{-4}$.

To determine changes in energy spread at low RF voltages is pretty challenging because the slope gets smaller with lower V_{RF}. Increasing the RF voltage allows us to observe several thresholds as the energy spread slope becomes bigger. From Fig. 7 we can clearly see multiple thresholds as a function of single bunch current.

The same threshold behaviour can be seen from the bunch lengthening simulations (Fig. 8). The resolution to determine the thresholds gets higher with the RF voltage. Here we show the maximum value of the bunch length during the unstable motion above the microwave instability threshold (I_{th1}. The bunch length is constant, yet current dependent, below I_{th1}.

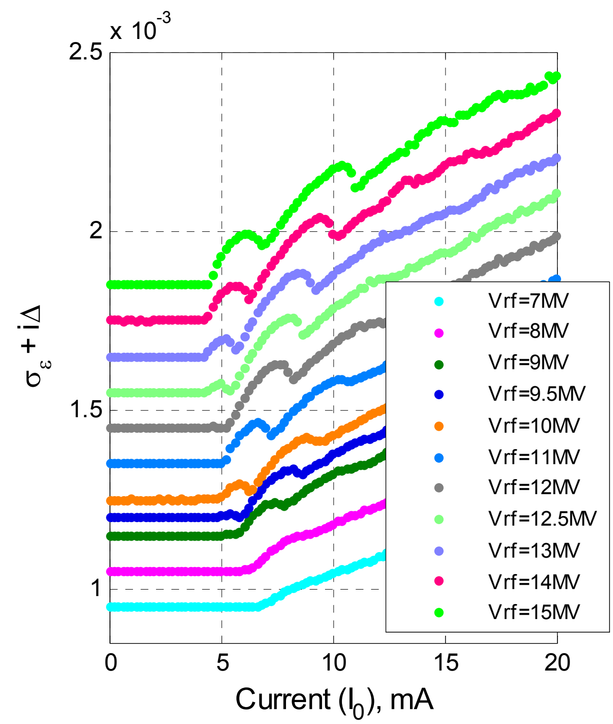

Figure 7: SPACE simulations of the energy spread (σ_ε) vs single bunch current (I_0) at different RF voltages. The vertical data are separated uniformly by quantity $\Delta = 1 \times 10^{-4}$ for $n = 0,1,2,..9$ for better observation of the changes in the thresholds behaviour.

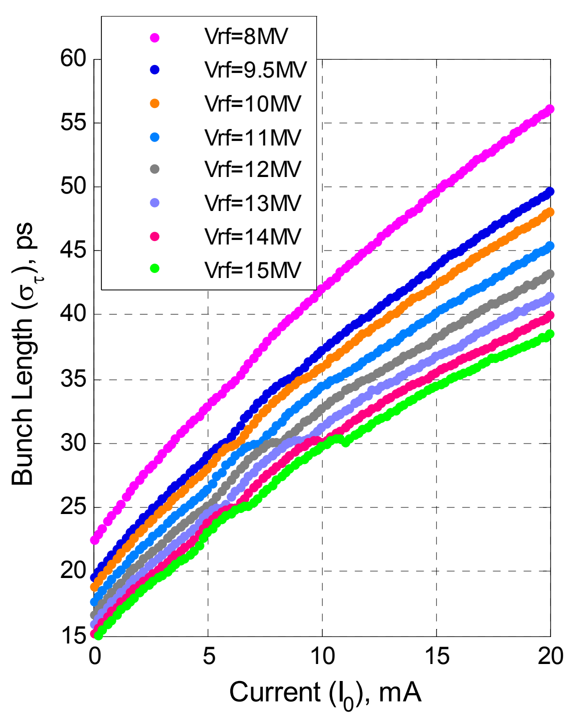

Figure 8: SPACE simulations of the bunch length (σ_τ) vs single bunch current (I_0) at different RF voltages.

As a brief summary, in Fig. 9 we plot the longitudinal instability thresholds map vs. RF voltage. From Fig. 7, we can identify the first microwave instability threshold I_{th1} (red dots) and several other instability thresholds at different single-bunch current.

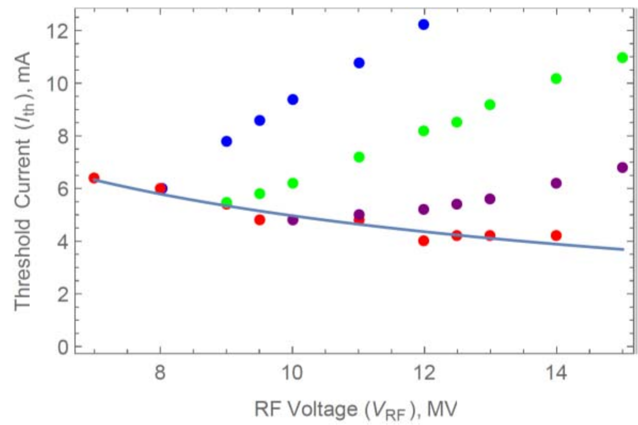

Figure 9: Summary of the simulated data for the longitudinal instability thresholds vs the RF voltage.

CONCLUSION

Both codes, ELEGANT and SPACE, demonstrate capability to simulate accurately the collective longitudinal beam instabilities with known wakepotential and parameters of the storage ring Multiple instability thresholds observed at APS have been confirmed by simulations.

REFERENCES

[1] M. Borland, "elegant: A Flexible SDDS-Compliant Code for Accelerator Simulation," Argonne National Laboratory, ANL/APS/LS-287, 2000.

[2] G. Bassi, A. Blednykh, and V. Smaluk, "Self-consistent simulations and analysis of the coupled-bunch instability for arbitrary multi-bunch configurations," *Phys. Rev. Accel. Beams*, vol. 19, p. 024401, 2016.

[3] M. Borland, G. Decker, L. Emery, W. Guo, K. Harkay, V. Sajaev, C.-Y. Yao, "APS Storage Ring Parameters," `http://www.aps.anl.gov/Accelerator_Systems_Division/Accelerator_Operations_Physics/SRparameters/`.

[4] W. Bruns, `http://www.gdfidl.de`

[5] R. R. Lindberg, "Instability Thresholds for the Advanced Photon Source Multi- Bend Achromat Upgrade" in *Proc. IPAC'15*, Richmond, VA, USA, May 2015, pp. 1822-1824.

[6] Y.-C. Chae, L. Emery, A.H. Lumpkin, J. Song, B.X. Yang, "Measurement of the Longitudinal Microwave Instability in the APS Storage Ring," in *Proc. PAC'01*, Chicago, IL, USA, Jun. 2001, pp. 1817-1819.

[7] APS, `http://www.aps.anl.gov/Accelerator_Systems_Division/Accelerator_Operations_Physics/SRparameters/node6.html`

[8] P.B. Wilson *et al.*, "Bunch Lengthening and Related Effects in SPEAR II," *IEEE Trans. Nucl. Sci.*, vol. 24, no. 3, p. 1211, 1977.

[9] A. Blednykh, B. Bacha, G. Bassi, W. Cheng, O. Chubar, Y.-C. Karen, V. Smaluk, "Microwave Instability Studies in NSLS-II," presented at NAPAC16, Chicago, IL, USA, Oct. 2016, paper WEA1CO05, this conference.